Book of Abstracts

Influence of mass lumping techniques on contact pressure oscillations in explicit finite element contact-impact algorithm based on isogeometric analysis with NURBS

J. Kopačka, D. Gabriel, J. Plešek and R. Kolman

Abstract Artificial oscillations in the contact pressure due to non-smooth contact surface are treated by the isogeometric analysis (IGA). After a brief overview of the B-splines and NURBS representations, an explicit finite element (FE) contact-impact algorithm is presented in a small deformation context. Contact constraints are regularized by the penalty method. The contact-impact algorithm is tested by means of dynamic Hertz problem. The classic FEA solution is compared with the IGA solution while different mass lumping techniques are considered.

1 Introduction

The main difficulty in the contact analysis is non-smoothness. It arises from unilateral contact constraints as well as geometric discontinuities inducted by the spatial discretization. The contact analysis based on traditional finite elements utilizes element facets to describe contact surfaces. The facets are C^0 continuous so that surface normal vectors can experience jump across facet boundaries leading to artificial oscillations in contact forces.

There were attempts to treat geometric discontinuities by smoothing contact surfaces using a splines interpolation. These remedies introduce an additional geometry on the top of the existing finite element mesh. It also adds an additional layer of data management and increases computational overhead. Details and further references can be found in [17].

Another remedy to overcome this geometric discontinuity may provides isogeometric analysis (IGA) [7]. In this approach, known geometry is accurately described by Non-Uniform Rational B-Splines (NURBS) basis functions which serve at the same time as element shape functions. The isogeometric analysis provides some additional advantage, which is especially attractive to the contact analysis, namely,

Institute of Thermomechanics AS CR, v. v. i., Dolejškova 1402/5, 182 00 Praha 8, Czech Republic, e-mail: {kopacka|gabriel|plesek|kolman}@it.cas.cz

preserving geometric continuity, facilitating patch-wise contact search, supporting a variationally consistent formulation, and having a uniform data structure for contact surfaces and underlying volumes.

Sharp corners or C^0 edges that can exist on the interface of two patches present a challenge to contact detection. A strategy to seamlessly deal with sharp corners was proposed in [11]. Here, unilateral contact constraints were regularized by the penalty method and the contact virtual work was discretized by the finite strain surface-to-surface contact element. Both one-pass and two-pass contact algorithms were tested.

In Reference [15], finite deformation frictionless quasi-static thermomechanical contact problems were considered. In this work, two penalty-based contact algorithms were studied. The former one was called knot-to-surface (KTS) algorithm. It is the straightforward extension of the classic node-to-surface (NTS) algorithm. Since the NURBS control points are not interpolatory, contact constraints were enforced directly at the quadrature points. It was shown that this approach is over-constrained and therefore not acceptable if a robust formulation with accurate tractions is desired. The latter one was called mortar-KTS algorithm. In this algorithm a mortar projection to control point pressures was employed to obtain the correct number of constraints.

The penalty-based mortar-KTS algorithm was extended to frictional contact in References [9] and [16]. The mortar-KTS algorithm was also studied in conjugation with augmented Lagrangian method in [10]. Isogeometric frictionless contact analysis using non-conforming mortar method in two-dimensional linear elasticity regime was presented in [8].

This paper is devoted to application of the NURBS based isogeometric analysis to contact-impact problems. After a brief overview of the B-Splines and NURBS representation in Section 2, the linear elastodynamics contact initial/boundary value problem is formulated in Section 3. The variational formulation in Section 4 serves as the base of finite element discretization, which is described in Section 5. Then, an explicit time integration scheme and several mass lumping techniques are described in Section 6 and 7, respectively. The presented IGA contact-impact algorithm is demonstrated on dynamic Hertz problem in Section 8. The conclusions are drawn in Section 9.

2 B-splines and NURBS

This section gives a brief overview of the main principle of the B-spline and NURBS representation. For more detailed description as well as efficient algorithms see, e.g. [13]. Throughout this paper we use p to indicate the polynomial degree, n to indicate the number of basis functions, d_{p} to indicate the number of parametric dimensions, and d_{s} to indicate the number of spatial dimensions.

A B-spline or NURBS object is called patch. The patch is parametrized by the linear combination of control points $\mathbf{P}_A \in \Re^{d_{\mathrm{s}}}$ and basis functions $N_A(\xi) : \Re^{d_{\mathrm{p}}} \mapsto$

$[0,1]$. A particular B-splines/NURBS basis function is defined with the aid of the so called knot vector

$$\Xi^i = \left\{ \underbrace{\xi^i_1,\ldots,\xi^i_{p_i+1}}_{p_i+1 \text{ equal terms}}, \xi^i_{p_i+2},\ldots,\xi^i_{n_i}, \underbrace{\xi^i_{n_i+1},\ldots,\xi^i_{n_i+p_i+1}}_{p_i+1 \text{ equal terms}} \right\}, \quad i=1,\ldots d_{\mathrm{p}} \tag{1}$$

The knot vector is a non-decreasing sequence of parametric coordinates. The knot vector is said to be uniform if the knots are unequally spaced in the parametric space. If the first and the last knot value appears p_i+1 times, the knot vector is called open. The B-spline/NURBS object with open knot vectors are interpolatory at the corner of a patch. It means that the boundary of a B-spline/NURBS object, with d_{p} parametric dimensions, is itself a B-spline/NURBS object with $d_{\mathrm{p}}-1$ dimensions.

The B-spline basis functions are defined by the Cox-de Boor recursion formula. It holds for $p=0$

$$N_{j,0}(\xi) = \begin{cases} 1 & \xi \in \left[\xi_j, \xi_{j+1}\right), j=1\ldots n \\ 0 & \text{otherwise} \end{cases} \tag{2}$$

and for $p>0$

$$N_{j,p}(\xi) = \frac{\xi-\xi_j}{\xi_{j+p}-\xi_j} N_{j,p-1}(\xi) + \frac{\xi_{j+1+p}-\xi}{\xi_{j+1+p}-\xi_{j+1}} N_{j+1,p-1}(\xi) \tag{3}$$

The B-splines are known to be unable to exactly describe some curves. NURBS was developed to extend interpolatory capability of the B-splines. The extension originates from projection geometry of conic sections. More details can be found in [13]. The p^{th} degree NURBS basis function is defined by

$$R^p_j(\xi) = \frac{N_{j,p}(\xi) w_j}{\sum_{\hat{j}=1}^{n} N_{\hat{j},p}(\xi) w_{\hat{j}}} \tag{4}$$

where w_j is referred to as the j^{th} weight.

Multivariate NURBS objects can be constructed simply by tensor product of univariate NURBS basis functions (4). For $d_{\mathrm{p}}=2$

$$R^{p_1,p_2}_{j_1,j_2}(\xi^1,\xi^2) = R^{p_1}_{j_1}(\xi^1) \otimes R^{p_2}_{j_2}(\xi^2) = \frac{N_{j_1,p_1}(\xi^1) N_{j_2,p_2}(\xi^2) w_{j_1,j_2}}{\sum_{\hat{j}_1=1}^{n_1} \sum_{\hat{j}_2=1}^{n_2} N_{\hat{j}_1,p_1}(\xi^1) N_{\hat{j}_2,p_2}(\xi^2) w_{\hat{j}_1,\hat{j}_2}} \tag{5}$$

and similarly for higher parametric dimensions.

With NURBS basis functions at hand we can introduce surface discretization by

$$\mathbf{x}(\xi^1,\xi^2) = \sum_{j_1=1}^{n_1} \sum_{j_2=1}^{n_2} R^{p_1,p_2}_{j_1,j_2}(\xi^1,\xi^2) \mathbf{P}_{j_1,j_2} \tag{6}$$

where $\mathbf{P}_{j_1,j_2} \in \Re^{d_s}$ is the control net, i.e., array of coordinates of control points. Adopting the isogeometric concept, an analogous interpolation is used for unknown displacement field and its variation. Utilizing proper connectivity arrays according to [4], one can write

$$\mathbf{x}(\xi) = \sum_{A=1}^{n_{\mathrm{cp}}} R_A(\xi)\mathbf{x}_A \qquad \mathbf{u}(\xi) = \sum_{A=1}^{n_{\mathrm{cp}}} R_A(\xi)\mathbf{u}_A \qquad \delta\mathbf{u}(\xi) = \sum_{A=1}^{n_{\mathrm{cp}}} R_A(\xi)\delta\mathbf{u}_A \tag{7}$$

where $\xi \in \Re^{d_\mathrm{p}}$ is the vector of isoparametric coordinates, A is the index of global basis function, which is related to indices of univariate basis function by the connectivity array $A = \mathtt{INC}(j_1, j_2, \ldots, j_{d_\mathrm{p}})$, and n_{cp} is the number of control points.

3 Contact initial/boundary value problem

The problem of linear elastodynamics is governed by the balance of linear momentum

$$\nabla \cdot \boldsymbol{\sigma}(\mathbf{u}) + \mathbf{b} = \rho\ddot{\mathbf{u}}(\mathbf{x},t) \quad \text{in } \Omega \times \mathbb{I} \tag{8}$$

where $\Omega = \bigcup_i \Omega_i, i = 1,2$ is the set of spatial points, $\mathbf{x} \in \Re^{d_s}$, defining the contacting bodies, $\mathbb{I} = (0,T)$ is the time domain, $\mathbf{u}$ is the displacement field, $\mathbf{b}$ are the body forces and $\boldsymbol{\sigma}$ is the stress field, see Fig. 1. The superimposed dots denote the time derivatives. In linear elasticity the stress field can be computed from the engineering strain field

$$\boldsymbol{\varepsilon} = \frac{1}{2}\left((\nabla\mathbf{u})^{\mathrm{T}} + \nabla\mathbf{u}\right) \tag{9}$$

via Hooke's law

$$\boldsymbol{\sigma} = \mathbf{c} : \boldsymbol{\varepsilon} \tag{10}$$

where $\mathbf{c}$ is the tensor of elastic constants given as

$$\mathbf{c} = \lambda\mathbf{I}\otimes\mathbf{I} + 2\mu\mathbf{I} \tag{11}$$

where $\mathbf{I}$ is the second-order identity tensor and λ, μ are the Lamé constants. The problem is in general subject to certain initial and boundary conditions as well. The initial conditions

$$\mathbf{u}(\mathbf{x},0) = \mathbf{u}_0 \quad \text{in } \bar{\Omega} \tag{12}$$

$$\dot{\mathbf{u}}(\mathbf{x},0) = \mathbf{v}_0 \quad \text{in } \bar{\Omega} \tag{13}$$

are prescribed in the closure of domain $\bar{\Omega}$. The displacement and traction boundary conditions

$$\mathbf{u} = \bar{\mathbf{u}} \quad \text{on } \Gamma_{\mathrm{u}} \tag{14}$$

$$\boldsymbol{\sigma}\cdot\mathbf{n} = \bar{\mathbf{t}} \quad \text{on } \Gamma_{\sigma} \tag{15}$$

are prescribed on the $\Gamma_{\mathrm{u}} \subset \Gamma$ and $\Gamma_{\sigma} \subset \Gamma$, respectively; Γ denotes the boundary of the domain Ω; $\bar{\mathbf{u}}$ and $\bar{\mathbf{t}}$ are the prescribed displacements and tractions, respectively; the vector $\mathbf{n}$ stands for the outward normal vector to Γ.

Further, the contact constraints are described on the contact boundary $\Gamma_{\mathrm{c}} \subset \Gamma$ by the Signorini-Hertz-Moreau conditions

$$g_{\mathrm{N}} \leq 0, \quad t_{\mathrm{N}} = \boldsymbol{\sigma} \cdot \mathbf{n} \leq 0, \quad g_{\mathrm{N}} t_{\mathrm{N}} = 0, \quad \text{on } \Gamma_{\mathrm{c}} \tag{16}$$

also known as the Karush-Kuhn-Tucker (KKT) conditions. Here, the normal gap function g_{N} has been introduced as

$$g_{\mathrm{N}} = -(\mathbf{x}_2 - \bar{\mathbf{x}}_1) \cdot \bar{\mathbf{n}}_1 \tag{17}$$

This definition is apparent from Fig. 1, where $\bar{\mathbf{x}}_1$ is the closest point projection of the point $\mathbf{x}_2$, lying on the contact boundary of body Ω_2, onto the contact boundary of body Ω_1. Note that the projected quantities are denoted by $(\bar{\bullet})$.

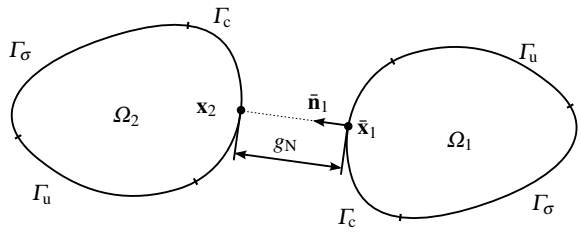

Fig. 1 Definition of the normal gap function.

The first inequality $(16)_1$ is called the impenetrability condition. The second condition $(16)_2$ asserts the negative traction vector, i.e. pressure, on the active contact boundary. It should be noted that the active contact boundary is considered such boundary, where the impenetrability condition is violated. Finally the third equality $(16)_3$, which is called the complementarity condition, ensures the complementarity between the gap function and the contact traction vector.

4 Variational formulation

In order to perform the finite element discretization, it is necessary to reformulate the strong form of the contact initial/boundary value problem in a weak sense. Hamilton's principle is a simple yet powerful tool that can be employed to derive the discretized system of equations. It states that of all admissible time histories of displacement field, the solution is one which minimizes the action functional

$$\mathbf{u} = \arg\min \left(\int_0^T \mathscr{L}\left(\mathbf{u}, \dot{\mathbf{u}}\right) \mathrm{d}t \right) \quad \text{subjected to } g_{\mathrm{N}} \geq 0 \text{ on } \Gamma_{\mathrm{c}} \tag{18}$$

where the Lagrangian functional, $\mathscr{L}(\mathbf{u}, \dot{\mathbf{u}})$, is defined as

$$\mathscr{L}\left(\mathbf{u}, \dot{\mathbf{u}}\right) = \mathscr{T}\left(\dot{\mathbf{u}}\right) - \left(\mathscr{U}\left(\mathbf{u}\right) - \mathscr{W}\left(\mathbf{u}\right)\right) \tag{19}$$

where

$$\mathscr{T}\left(\dot{\mathbf{u}}\right) = \int_{\Omega} \frac{1}{2} \rho \dot{\mathbf{u}} \cdot \dot{\mathbf{u}} \, \mathrm{d}V \tag{20}$$

$$\mathscr{U}\left(\mathbf{u}\right) = \int_{\Omega} \frac{1}{2} \boldsymbol{\sigma} : \boldsymbol{\varepsilon} \, \mathrm{d}V \tag{21}$$

$$\mathscr{W}\left(\mathbf{u}\right) = \int_{\Omega} \mathbf{u} \cdot \mathbf{b} \, \mathrm{d}V + \int_{\Gamma_{\sigma}} \mathbf{u} \cdot \bar{\mathbf{t}} \, \mathrm{d}S \tag{22}$$

are the kinetic energy, the strain energy, and the work done by external forces, respectively.

4.1 Penalty method

The penalty method is the simplest manner how to enforce unilateral contact constraints (16). The principle of the method is as follow. An extra term is added to the strain energy (21)

$$\mathscr{U}_{\mathrm{p}}\left(\mathbf{u}\right) = \int_{\Omega} \frac{1}{2} \boldsymbol{\sigma} : \boldsymbol{\varepsilon} \, \mathrm{d}V + \int_{\Gamma_{\mathrm{c}}} \frac{1}{2} \varepsilon_{\mathrm{N}} \left\langle g_{\mathrm{N}} \right\rangle^2 \mathrm{d}S \tag{23}$$

where $\langle \bullet \rangle$ stands for the Macaulay brackets which returns zero if the argument is negative (i.e. gap is open), otherwise it returns the argument itself. Now, the definition of the normal gap function (17) should be apparent. Further, the penalized Lagrangian functional is defined as

$$\mathscr{L}_{\mathrm{p}}(\mathbf{u}, \dot{\mathbf{u}}) = \mathscr{T}\left(\dot{\mathbf{u}}\right) - \left(\mathscr{U}_{\mathrm{p}}(\mathbf{u}) - \mathscr{W}(\mathbf{u})\right) \tag{24}$$

The unknown displacement field is sought as one which renders the penalized action functional stationary

$$\delta \int_0^T \mathscr{L}_{\mathrm{p}}\left(\mathbf{u}, \dot{\mathbf{u}}\right) \mathrm{d}t = 0 \tag{25}$$

where δ denotes the first Gateaux variation in the direction of virtual displacement $\delta\mathbf{u}$. Using the standard procedures one arrives to the principle of virtual displacements

$$\int_{\Omega} \rho \delta \mathbf{u} \cdot \ddot{\mathbf{u}} \, \mathrm{d}V + \int_{\Omega} \delta \boldsymbol{\varepsilon} : \boldsymbol{\sigma} \, \mathrm{d}V + \int_{\Gamma_{\mathrm{c}}} \delta g_{\mathrm{N}} \varepsilon_{\mathrm{N}} \left\langle g_{\mathrm{N}} \right\rangle \mathrm{d}S = \int_{\Omega} \delta \mathbf{u} \cdot \mathbf{b} \, \mathrm{d}V + \int_{\Gamma_{\sigma}} \delta \mathbf{u} \cdot \mathbf{t} \, \mathrm{d}S \tag{26}$$

which serves the base for the finite element discretization. The integrals in Equation (26) represent the virtual work of the inertia forces, internal forces, contact forces, body forces, and traction forces, respectively.

5 Finite element discretization

Applying the finite element discretization to the variational formulation (26) introduces the system of nonlinear ordinary differential equations

$$\mathbf{M}\ddot{\mathbf{u}} + \mathbf{K}\mathbf{u} + \mathbf{R}_{\mathrm{c}}(\mathbf{u}, \ddot{\mathbf{u}}) = \mathbf{R} \tag{27}$$

Here, $\mathbf{M}$ is the mass matrix, $\mathbf{K}$ is the stiffness matrix, $\mathbf{R}_{\mathrm{c}}$ is the contact residual vector, which is the source of nonlinearity, and $\mathbf{R}$ is the time-dependent load vector. Further, $\mathbf{u}$ and $\ddot{\mathbf{u}}$ contain nodal displacements and accelerations, respectively. The element mass and stiffness matrices are given by

$$\mathbf{M}_e = \int_{\Omega_e} \rho \mathbf{N}^{\mathrm{T}} \mathbf{N} \, \mathrm{d}V \qquad \mathbf{K}_e = \int_{\Omega_e} \mathbf{B}^{\mathrm{T}} \mathbf{C} \mathbf{B} \, \mathrm{d}V \tag{28}$$

where $\mathbf{C}$ is the elasticity matrix, $\mathbf{B}$ is the strain-displacement matrix, and $\mathbf{N}$ is the matrix which stores shape functions. Note that the integration is carried over the element domain Ω_e. Global matrices are assembled in the usual fashion.

In classic FEA, the shape functions are commonly chosen as Lagrange polynomials, whereas in IGA, the shape functions arise from the restriction of the NURBS basis function on the knot span, as was described in Section 2. The knot span is IGA equivalent of the finite element.

Motivated by the desire to preserve the symmetry, we proposed the contact residual vector in the form [5]

$$\mathbf{R}_{\mathrm{c}}(\mathbf{u}) = \int_{\Gamma_{\mathrm{c}_1}} \varepsilon_{\mathrm{N}} \mathbf{N}^{\mathrm{T}} g_{\mathrm{N}} \, \mathrm{d}S + \int_{\Gamma_{\mathrm{c}_2}} \varepsilon_{\mathrm{N}} \mathbf{N}^{\mathrm{T}} g_{\mathrm{N}} \, \mathrm{d}S \tag{29}$$

It should be noted that a similar idea was advocated also in work of Papadopoulos et al. [12], where the contact problem of two deformable bodies was treated as two interacting Signorini problems. Recently, this form of the contact residual vector was revitalized in the work of Sauer and De Lorenzis [14] and was called two-half-pass contact algorithm.

6 Explicit time integration

We now consider the time integration of the semi-discretized system (27) by the central difference method (CDM) [2]. First let the time interval $\mathbb{I}$ is subdivided to

$\bigcup_{n=0}^{N}[t_n, t_{n+1}]$ with the time step $\Delta t = t_{n+1} - t_n$. Further, let the displacement vectors $\mathbf{u}_{n-1}$ and $\mathbf{u}_n$ at time instances t_{n-1} and t_n, respectively, are known. Then one can calculate new displacement vector $\mathbf{u}_{n+1}$ at time t_n from the system of governing equations

$$\mathbf{M}\mathbf{a}_n = \mathbf{R}_n - \mathbf{K}\mathbf{u}_n - \mathbf{R}_{\mathrm{c}}^n \tag{30}$$

where the acceteration vector $\mathbf{a}_n$ is given by the central difference

$$\mathbf{a}_n = \frac{\mathbf{v}_{n+\frac{1}{2}} - \mathbf{v}_{n-\frac{1}{2}}}{\Delta t} \tag{31}$$

and where the velocity vectors are given by differences

$$\mathbf{v}_{n+\frac{1}{2}} = \frac{\mathbf{u}_{n+1} - \mathbf{u}_n}{\Delta t} \qquad \mathbf{v}_{n-\frac{1}{2}} = \frac{\mathbf{u}_n - \mathbf{u}_{n-1}}{\Delta t} \tag{32}$$

Due to possible non-smoothness of contact residual vector, $\mathbf{R}_{\mathrm{c}}^n$, in time interval $[t_n, t_{n+1}]$, it is advantageous to recast (30) into a predictor-corrector form [18]. In the predictor phase, a new displacement vector is computed regardless contact forces

$$\mathbf{a}_{\mathrm{pre}}^n = \mathbf{M}^{-1}(\mathbf{R}_n - \mathbf{K}\mathbf{u}_n) \tag{33}$$

$$\mathbf{v}_{\mathrm{pre}}^{n+\frac{1}{2}} = \mathbf{v}^{n-\frac{1}{2}} + \Delta t\,\mathbf{a}_{\mathrm{pre}}^n \tag{34}$$

$$\mathbf{u}_{\mathrm{pre}}^{n+1} = \mathbf{u}^n + \Delta t\,\mathbf{v}_{\mathrm{pre}}^{n+\frac{1}{2}} \tag{35}$$

where $\mathbf{a}_{\mathrm{pre}}^n$ is the predictor of acceleration, $\mathbf{v}_{\mathrm{pre}}^{1+\frac{1}{2}}$ is the predictor of velocity, and $\mathbf{u}_{\mathrm{pre}}^{n+1}$ is the predictor of displacement. The last mentioned is utilized to calculate the predictor configuration, in which the contact residual vector is evaluated. The final displacement vector is obtained throught the correction of acceleration and velocity

$$\mathbf{a}_{\mathrm{cor}}^n = \mathbf{M}^{-1}\mathbf{R}_{\mathrm{c}}^{n+1} \tag{36}$$

$$\mathbf{a}^n = \mathbf{a}_{\mathrm{pre}}^n + \mathbf{a}_{\mathrm{cor}}^n \tag{37}$$

$$\mathbf{v}^{n+\frac{1}{2}} = \mathbf{v}_{\mathrm{pre}}^{n+\frac{1}{2}} + \Delta t\,\mathbf{a}_{\mathrm{cor}}^n \tag{38}$$

$$\mathbf{u}^{n+1} = \mathbf{u}^n + \Delta t\,\mathbf{v}^{n+\frac{1}{2}} \tag{39}$$

7 Mass lumping techniques

The mass matrix calculated according to $(28)_1$ is called the consistent mass matrix. In general, such a mass matrix is not diagonal. It is obvious that the diagonal mass matrix entails significant computational savings and storage advantages. In this section most used techniques that produce diagonally lumped mass matrices are summarized.

Generally, the mass matrix must satisfy certain conditions: matrix symmetry, physical symmetries, conservation and positivity. Therefore, the diagonal components of the lumped mass matrix must be positive. Furthermore, the masses corresponding to the corner nodes and the masses corresponding to the midside nodes coincides for the square quadratic finite element. The condition for the keeping of the total element mass of the 8-node serendipity square finite element takes on the simple form

$$m = 4m_1 + 4m_2 \tag{40}$$

where m_1 denotes the mass of the midside node and m_2 is the mass of the corner node. If the mass corresponding to the midside node m_1 is chosen in the proportion to the total element mass m

$$m_1 = \alpha m \tag{41}$$

then for the mass of the corner node m_2 from the condition (40) holds

$$m_2 = (0.25 - \alpha)m \tag{42}$$

where α is the mass parameter. The value of the mass parameter α should be choosen in the range $[0, 0.25]$ requiring the positive definitness of the mass matrix. The value $\alpha = 8/36$ corresponds to the HRZ procedure [6] with 2×2 Gauss quadrature, $\alpha = 16/76$ the HRZ procedure with 3×3 Gauss quadrature and $\alpha = 1/3$ to the row sum method. Note that the limit mass distribution occurs for $\alpha = 0$ when full mass is inserted in the corner nodes and $\alpha = 0.25$ when full mass is concentrated in the midside nodes.

8 Dynamic Hertz problem

In this section, an example is presented to illustrate the performance of the classic FEA and IGA contact-impact algorithm described in the previous sections. The example deals with Hertz dynamic problem, a classical benchmark for which an analytical solution is available [3]. In the example, the effect of mass lumping is investigated. The analysis is limited to the second order elements. In particular, quadratic serendipity eight-node finite elements are used in case of FEA, and second order basis function in case of IGA.

The presented numerical example deals with frictionless impact of the cylinders of radius $R = 4\,\mathrm{m}$, see Fig. 2. The material of each of the cylinders is linearly elastic with Young's modulus $E = 1000\,\mathrm{MPa}$, Poisson's ratio $\nu = 0.2$, and density $\rho = 1\,\mathrm{kg}\cdot\mathrm{m}^3$. The initial velocity of the cylinders is $2\,\mathrm{m}\cdot\mathrm{s}^{-1}$. In the initial configuration the cylinders just touches each other in a point. Due to symmetry, only the half of each cylinder is considered. The penalty parameter is $\varepsilon_\mathrm{N} = 1 \times 10^5\,\mathrm{N}\cdot\mathrm{m}^{-2}$. The explicit time integration by CDM is performed for $0.9\,\mathrm{s}$ with the time step $5 \times 10^{-4}\,\mathrm{s}$. It should be noted that only one mesh is considered. The effect of mesh refinement will be study in the further work.

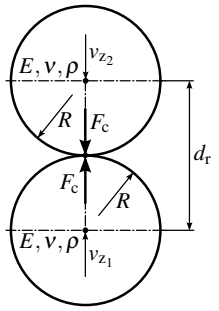

Fig. 2 Dynamic Hertz problem.

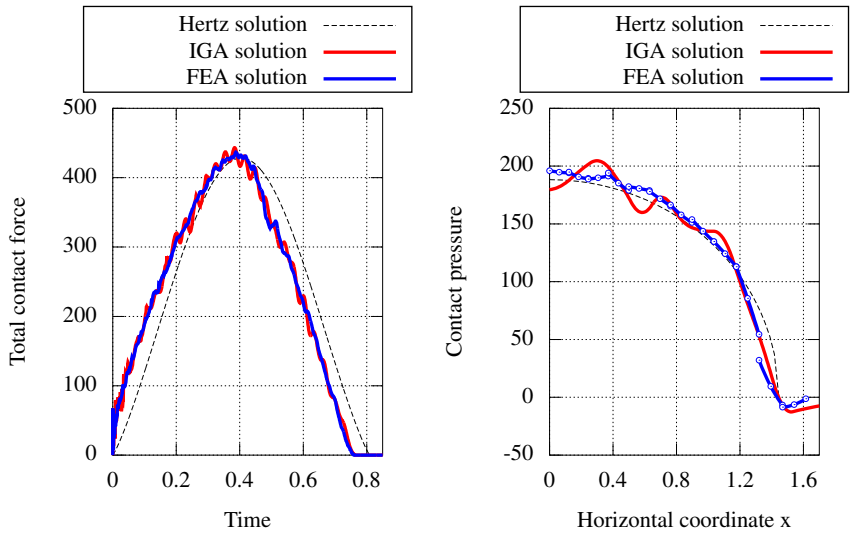

Fig. 3 Comparison of classic FEA and IGA solution of contact forces (left) and contact pressures (right) for HRZ mass lumping method.

Fig. 3 shows the contact force and the maximal contact pressure obtained for both FEA and IGA with HRZ mass lumping technique. The HRZ method was chosen because in case of second order Lagrange elements the row sum method leads to negative mass on diagonal, which is not admissible. The results show a good agreement with the analytical solution. One can notice that the FEA solution in comparison with IGA solution exhibits lower oscillations.

In order to evaluate the effect of mass lumping techniques on the oscillations of the contact forces and contact pressure distribution in IGA, further analyses are performed using consistent mass matrix and mass matrix lumped by the row sum method. Fig. 4 shows that consistent mass matrix delivers a more accurate contact pressure distribution than row sum and HRZ mass lumping techniques.

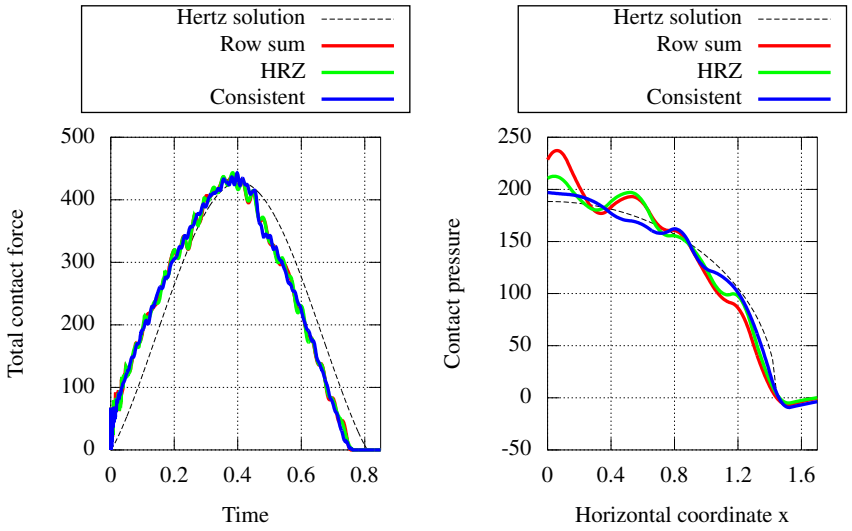

Fig. 4 Influence of mass lumping techniques on contact forces (left) and contact pressures (right) for IGA.

9 Conclusions

This paper addressed the utilization of the NURBS based isogeometric analysis in an explicit contact-impact algorithm. Two main conclusions may be drawn:

- For second order elements and mass matrix lumped by the HRZ method, IGA in comparison with classic FEA leads to a more oscillatory contact force and consequently also contact pressure.
- The oscillations of the contact forces in IGA are minimal for consistent mass matrix.

Nevertheless, employing the consistent mass matrix in the explicit integration causes decrease of efficiency. An interesting alternatives could be the isogeometric collocation method [1], which is known to lead to diagonal mass matrix. It will be the object of the further investigations.

Acknowledgments

Acknowledgements to GAP101/12/2315 with institutional support RVO:61388998.

References

1. Auricchio, F., Beirão da Veiga, L., Hughes, T.J.R., Reali, A., Sangalli, G.: Isogeometric collocation for elastostatics and explicit dynamics. Computational Methods in Applied Mechanics and Engineering **249–252**, 2–14 (2012). DOI 10.1016/j.cma.2012.03.026
2. Belytschko, T., Liu, W.K., Moren, B.: Nonlinear Finite Element for Continua and Structures. John Wiley & Sons, Ltd (2000)
3. Chandrasekaran, N., Haisler, W.E., Goforth, R.E.: A finite element solution method for contact problems with friction. International Journal for Numerical Methods in Engineering **24**(3), 477–495 (1987). DOI 10.1002/nme.1620240302
4. Cottrell, J.A., Hughes, T.J.R., Bazilevs, Y.: Isogeometric Analysis: Toward Integration of CAD and FEA. John Wiley & Sons (2009)
5. Gabriel, D., Plešek, J., Ulbin, M.: Symmetry preserving algorithm for large displacement frictionless contact by the pre-discetization penalty method. International Journal for Numerical Methods in Engineering **61**(15), 2615–2638 (2004). DOI 10.1002/nme.1173
6. Hinton, E., Rock, T., Zienkiewicz, O.C.: A note on mass lumping and related processes in the finite element method. Earthquake Engineering & Structural Dynamics **4**(3), 245–249 (1976). DOI 10.1002/eqe.4290040305
7. Hughes, T.J.R., Cottrell, J.A., Bazilevs, Y.: Isogeometric analysis: CAD, finite elements, NURBS, exact geometry and mesh refinement. Computer Methods in Applied Mechanics and Engineering **194**(39–41), 4135–4195 (2005). DOI 10.1016/j.cma.2004.10.008
8. Kim, J.Y., Youn, S.K.: Isogeometric contact analysis using mortar method. International Journal for Numerical Methods in Engineering **89**, 1559–1581 (2011). DOI 10.1002/nme.3300
9. Lorenzis, L.D., Temizer, I., Wriggers, P., Zavarise, G.: A large deformation frictional contact formulation using nurbs-based isogeometric analysis. International Journal for Numerical Methods in Engineering **87**, 1278–1300 (2011). DOI 10.1002/nme.3159
10. Lorenzis, L.D., Wriggers, P., Zavarise, G.: A mortar formulation for 3d large deformation contact using nurbs-based isogeometric analysis and the augmented lagrangian method. Computational Mechanics **49**, 1–20 (2012). DOI 10.1007/s00466-011-0623-4
11. Lu, J.: Isogeometric contact analysis: Geometric basis and formulation for frictionless contact. Comput. Methods Appl. Mech. Engrg. **200**, 726–741 (2010)
12. Papadopoulos, P., Jones, R.E., Solberg, J.M.: A novel finite element formulation for frictionless contact problems. International Journal for Numerical Methods in Engineering **38**, 2603–2617 (1995)
13. Piegl, L., Tiller, W.: The NURBS Book (Monographs in Visual Communication), 2 edn. Springer-Verlag (1997)
14. Sauer, R.A., Lorenzis, L.D.: A computational contact formulation based on surface potentials. Computational Methods in Applied Mechanics and Engineering **253**, 369–395 (2013)
15. Temizer, I., Wriggers, P., Hughes, T.J.R.: Contact treatment in isogeometric analysis with nurbs. Computational Methods in Applied Mechanics and Engineering **200**, 1100–1112 (2011). DOI 10.1016/j.cma.2010.11.020
16. Temizer, I., Wriggers, P., Hughes, T.J.R.: Three-dimensional mortar-based frictional contact treatment in isogeometric analysis with nurbs. Computational Methods in Applied Mechanics and Engineering **209–2012**, 115–128 (2012). DOI 10.1016/j.cma.2011.10.014
17. Wriggers, P.: Computational Contact Mechanics, 2nd edn. Springer (2006)
18. Wu, S.R.: A variational principle for dynamic contact with large deformation. Computational Methods in Applied Mechanics and Engineering **198**, 2009–2015 (2009)